Synchrotron X-ray Studies of $Al_{1-y}Ti_y$ Formation and Re-hydriding Inhibition in Ti-Enhanced $NaAlH_4$

Hendrik W. Brinks,*,† Bjørn C. Hauback,† Sesha S. Srinivasan,‡ and Craig M. Jensen‡

Institute for Energy Technology, P. O. Box 40, Kjeller, NO-2027 Norway, and Department of Chemistry, University of Hawaii, Honolulu, Hawaii 96822

Received: March 1, 2005; In Final Form: May 9, 2005

$NaAlH_4$ samples with Ti additives ($TiCl_3$, TiF_3, and $Ti(OBu)_4$) have been investigated by synchrotron X-ray diffraction in order to unveil the nature of Ti. No crystalline Ti-containing phases were observed after ball milling of $NaAlH_4$ with the additives, neither as a solid solution in $NaAlH_4$ nor as secondary phases. However, after cycling, a high-angle shoulder of Al is observed in the same position with 10% $TiCl_3$ as that with 2% $Ti(OBu)_4$, but with considerably higher intensity, indicating that the shoulder is caused by Ti. After prolonged reabsorption, there is only a small fraction of free Al phase left to react with Na_3AlH_6, whereas the shoulder caused by $Al_{1-y}Ti_y$ is dominating. The Ti-containing phase causing the shoulder therefore contains less Ti than Al_3Ti, and the aluminum in this phase is too strongly bound to react with Na_3AlH_6 to form $NaAlH_4$. The composition of the $Al_{1-y}Ti_y$ phase is estimated from quantitative phase analysis of powder X-ray diffraction data to be $Al_{0.85}Ti_{0.15}$. Formation of this phase may explain the reduction of capacity beyond the theoretical reduction from the dead weight of the additive and the reaction between the additive and $NaAlH_4$.

1. Introduction

The development of lightweight, high reversible capacity hydrogen storage materials is of central importance to the actualization of practical hydrogen-powered vehicles. In 1997, Bogdanovic and Schwickardi[1] reported that the elimination of hydrogen from solid $NaAlH_4$ is markedly accelerated and rendered reversible under moderate conditions upon mixing the hydride with a few mole percent of selected transition metal complexes. Since that time, aluminum-based complex hydrides, "alanates", have been regarded as a highly promising group of materials for onboard hydrogen-storage applications. Hydrogen cycling capacities of 3−4 wt % have been achieved for Ti-doped $NaAlH_4$ at 120−160 °C with relatively good kinetics.[2−5]

$NaAlH_4$ decomposes according to the three sequential steps seen in eqs 1−3. The first two reactions, releasing in total 5.6 wt % hydrogen, are regarded as useable for reversible hydrogen storage at moderately low temperatures. Two-thirds of this hydrogen is released in the first reaction.

$$NaAlH_4 = {}^1/_3Na_3AlH_6 + {}^2/_3Al + H_2 \quad (1)$$

$${}^1/_3Na_3AlH_6 = NaH + {}^1/_3Al + {}^1/_2H_2 \quad (2)$$

$$NaH = Na + {}^1/_2H_2 \quad (3)$$

Ti can be introduced into the hydride either by mixing $NaAlH_4$ with the Ti-based additive (often titanium halides) in a dispersion[1] or by ball milling.[6] Samples prepared in these ways have been studied, and partial results on the state of Ti have been achieved. For the former technique, hydrogen evolution during the reaction was determined in accordance with reduction of $Ti^{III/IV}$ to Ti^0 without changing the valence of Al.[7] ^{57}Fe Mössbauer spectroscopy investigations confirm formation of bcc Fe from addition of both $Ti(OBu)_4$ and $Fe(OEt)_2$ to $NaAlH_4$ and suggest formation of an Fe−Al alloy during dehydrogenation.[7]

For samples prepared by ball milling, recent X-ray absorption studies indicate Ti^0, at least after cycling of $NaAlH_4$ with Ti additives.[8−10] Thorough powder X-ray diffraction (PXD) studies of fresh and cycled $NaAlH_4$ samples with different additives do not indicate any significant bulk solid solution of Ti in Na or Al sites from precise determination of the unit-cell dimensions.[11,12] Neutron diffraction data, with intensities strongly dependent on an eventual solid solution of Ti in $NaAlD_4$, are in line with that.[11] No crystalline Ti-containing phases were detected in samples that were ball-milled but not cycled.[11,12] However, after cycling at least part of the Ti is forming a phase with Al after cycling with a lower Ti-content than Al_3Ti.[11] The content of this Ti−Al phase has been reported to increase with increasing Ti additive.[13] Similar observations were made in studies of the synthesis of $TiAl_3$ from a suspension of $TiCl_3$ and $LiAlH_4$ in mesitylene heated to 550 °C.[14] In this study, Al was detected by PXD in the precipitate before heating, but neither Ti nor any Ti−Al alloy were detected at this point. The main part of the Ti compounds added to $NaAlH_4$ is probably reduced to Ti^0 in the ball-milling process and forms an Al-rich Ti−Al alloy after the heat treatment during cycling. The fact that Ti−Al alloys can be prepared by ball milling of the elements[15−21] supports this hypothesis. However, still the mechanism of the enhancement of the kinetics is not revealed.

To further unveil the nature of the titanium species that arises from ball milling $NaAlH_4$ with titanium additives and perhaps hence extend the knowledge of the mechanism of the action of the additives, cycled samples with $TiCl_3$, TiF_3, and $Ti(OBu)_4$ additives were analyzed in detail by synchrotron radiation PXD (SR-PXD).

* To whom correspondence should be addressed. Telephone: +47 63 80 64 99. Fax: +47 63 81 09 20. E-mail: hwbrinks@ife.no.
† Institute for Energy Technology.
‡ University of Hawaii.

10.1021/jp051031p CCC: $30.25
Published on Web 07/30/2005

TABLE 1: Mole Fractions (%) of the Phases Based on Rietveld Refinements

sample no.	additive	no.of cycles	% $NaAlH_4$	% Na_3AlH_6	% $Al/Al_{1-y}Ti_y$	% NaCl
1	10% $TiCl_3$	0	58.9		22.4	18.7
2	10% $TiCl_3$	3	14.4	14.2	46.8	24.5
3[a]	10% TiF_3	0	59.0	4.4	36.6	
4	2% $Ti(OBu)_4$	101	71.9	5.9	19.8	2.0

[a] NaF was not observed.

TABLE 2: Unit-Cell Dimensions Determined by Rietveld Refinements of Synchrotron Radiation PXD Data of the Ti-Enhanced $NaAlH_4$ Samples

	$NaAlH_4$		Na_3AlH_6	Al	$Al_{1-y}Ti_y$
sample no.	a (Å)	c (Å)	V (Å^3)	a (Å)	a (Å)
1	5.0237(1)	11.3507(2)		4.0489(1)	
2	5.0234(1)	11.3514(2)	232.34(1)	4.0493(1)	4.0368(1)
3	5.0235(1)	11.3500(2)	232.50(2)	4.0493(1)	
4	5.0237(1)	11.3503(1)	232.39(1)	4.0490(-)	4.0344(4)

[a] Estimated standard deviations are given in parentheses. For comparison, the values for the pure phases determined at the same instrument are as follows: $a = 5.0232(1)$ Å and $c = 11.3483(1)$ Å for $NaAlH_4$, $V = 232.50(2)$ Å for Na_3AlH_6, and $a = 4.0490$ Å for Al.[11]

2. Experimental Section

All reactions and operations were performed under argon in a glovebox or using standard Schlenk techniques with oxygen and water free solvents. $NaAlH_4$ was purchased from Albemarle Corp. and recrystallized with THF/pentane before use. $TiCl_3$ and TiF_3 were purchased from Aldrich Chemicals Inc. and used without further purification. $TiCl_3$ and TiF_3 were added to $NaAlH_4$ by ball milling 30 and 60 min, respectively, in a Fritsch pulverizette 7 at 350 rpm. The ball to sample mass ratio was approximately 20:1.

The cycled samples with $TiCl_3$ were dehydrided at 160 °C against 1 bar pressure for 3 h and hydrided at 115 bar at 120 °C for 12 h. The $NaAlH_4$ with $Ti(OBu)_4$ additive was cycled 100 cycles with the same conditions (same sample as in ref 3), and the last rehydrogenation (cycle 101) was carried out at 85 bar and 120 °C for 65 h.

SR-PXD data at 22 °C were collected at the Swiss−Norwegian beam line (station BM1B) at the European Synchrotron Radiation Facility (ESRF) in Grenoble, France. The samples were kept in rotating 0.5 mm boron-silica-glass capillaries. Intensities were measured in steps of $\Delta(2\theta) = 0.004$ and 0.005°. The wavelength of 0.49956 Å was obtained from a channel-cut Si(111) monochromator.

Rietveld refinements were carried out using the program Fullprof (version 2.80).[22] X-ray form factors were taken from the Fullprof library. Thompson−Cox−Hastings pseudo-Voigt profile functions were used, and backgrounds were modeled by interpolation between manually chosen points. Information of the microstructure was obtained from isotropic broadening effects included in the Rietveld refinements. The instrumental resolution was determined with a LaB_6 standard.

3. Results

The samples that were analyzed by SR-PXD were $NaAlH_4$ with 10 mol % $TiCl_3$, uncycled (sample 1) and after 3 cycles (sample 2), 10 mol % TiF_3 uncycled (sample 3) and 2 mol % $Ti(OBu)_4$ (sample 4) after 101 cycles. The mole fractions of each phase present in the samples and selected unit-cell dimensions from the Rietveld refinements are shown in Tables 1 and 2, respectively.

The unit-cell dimensions of the samples do not deviate from the pure samples of $NaAlH_4$ and Na_3AlH_6. This is in line with earlier observations[11] and indicates that there is no significant solid solution of Ti in the alanate. In addition, no Ti-containing phases were observed in the uncycled samples. Hence, no conclusions can be drawn from SR-PXD on the state of Ti directly after ball milling. The fit of the Rietveld refinement of the uncycled sample 1 is shown in Figure 1.

The addition of $TiCl_3$ results in formation of crystalline Al and NaCl. The SR-PXD reflections from NaCl are very broad after ball milling, but after cycling they are significantly sharper; cf. Figure 2. On the basis of microstructural analysis of the SR-PXD data, the broadening was found to originate both from strain and small crystallite size. The crystallite size was estimated to increase from 11 nm after ball milling until 270 nm after 3 cycles. Hence, the heat treatment in the cycling process results in a considerable increased crystallite size for NaCl. Al is formed in the same reaction, but the reflections are much sharper and the change in half-width of the reflections during cycling is less pronounced. The crystallite sizes of Al and $NaAlH_4$ were estimated to 56 and 170 nm after ball milling, and the sizes increase during cycling. More details on the microstructure of Ti-enhanced $NaAlH_4$ will be given in a forthcoming paper.

The reaction can be assumed to be

$$NaAlH_4 + 0.1TiCl_3 = 0.7NaAlH_4 + 0.3NaCl + 0.3Al + 0.1\text{“Ti”}_{(am)} + 0.6H_{2(g)} \quad (4)$$

After normalization, the expected mole percent of the crystalline phases for this reaction is 53.8% $NaAlH_4$, 23.1% NaCl, and 23.1% Al. The refined values based on the SR-PXD data for sample 1 are 58.9, 18.7, and 22.4%, respectively. This indicates that eq 4 is a good approximation of the reaction when $NaAlH_4$ is ball-milled with 10% $TiCl_3$.

For the TiF_3-enhanced $NaAlH_4$ (sample 3), crystalline NaF is not formed as expected by analogy to eq 4. This was earlier observed for 6% TiF_3,[11] and even 10% is not enough to observe any NaF. The reason for this may be that the crystallite size is even smaller than for NaCl and it becomes below the detection limit of SR-PXD. The background is slightly elevated around the expected positions for the NaF reflections. Furthermore, preliminary in-situ SR-PXD experiments indicate that NaF is formed upon heating in a vacuum and that the reflections gradually sharpen by heating.

Small amounts of Na_3AlH_6 were observed after ball milling with TiF_3 (sample 3). By assuming the reaction

$$NaAlH_4 + 0.1TiF_3 = 0.7NaAlH_4 + 0.3Al + 0.3\text{“NaF”}_{(am)} + 0.1\text{“Ti”}_{(am)} + 0.6\,H_{2(g)} \quad (5)$$

and furthermore allowing partial thermal decomposition during ball milling according to eq 1, the amounts of the resulting phases can be estimated. Rietveld refinements of the SR-PXD data gave 4.4 mol % Na_3AlH_6. From eqs 5 and 1 this corresponds to 56.8 and 38.8 mol % of $NaAlH_4$ and Al, respectively. This fits very well with the observed values of

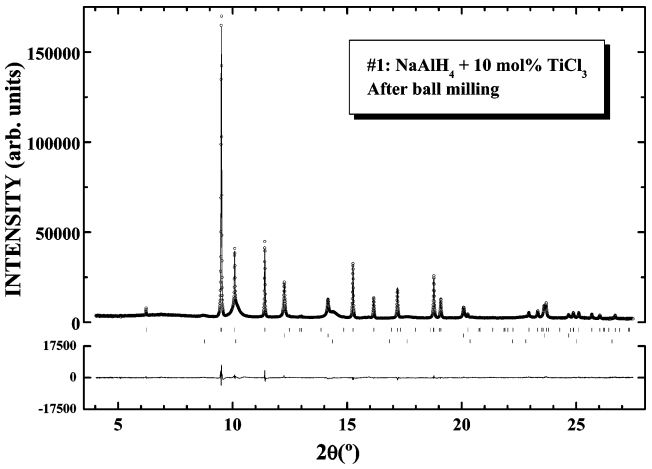

Figure 1. Observed intensities (circles) and calculated intensities from Rietveld refinements (upper line) of $NaAlH_4$ with 10 mol % $TiCl_3$ added ball milling, measured at 22 °C at BM1B, ESRF. Positions of Bragg reflections are shown with bars for $NaAlH_4$, Al, and NaCl (from top). The difference between observed and calculated intensity are shown with the bottom line.

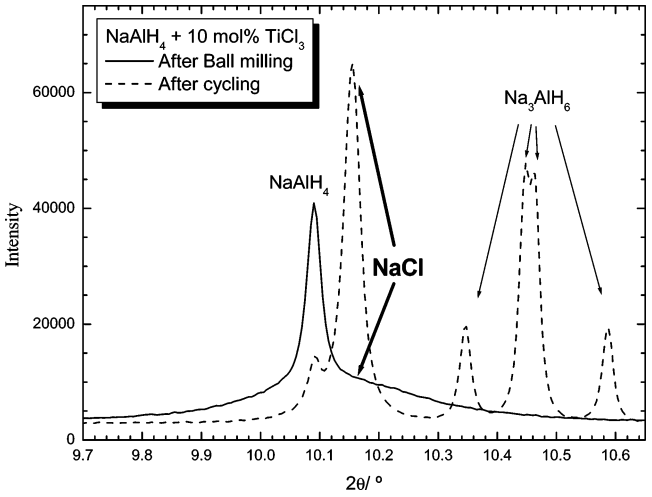

Figure 2. Comparison of the peak shape of NaCl in $NaAlH_4$ with 10 mol % $TiCl_3$ after ball milling and after cycling.

59.0 ($NaAlH_4$) and 36.6 mol % (Al). Hence, the "crystalline part" of eq 5 is confirmed, and the consumption of TiF_3 is fairly complete.

Quantitative phase analysis of the cycled sample of $NaAlH_4$ with 10 mol % $TiCl_3$ (sample 2), which was rehydrided in the final cycle, indicates equal amounts of $NaAlH_4$ and Na_3AlH_6; cf. Table 1. On the basis of eqs 4 and 1, the phase fractions can be estimated to be 13.5 ($NaAlH_4$), 13.5 (Na_3AlH_6), 50.0 (Al), and 23.0% (NaCl). These are close to the observed values: 14.4, 14.2, 46.8, and 24.5%, respectively. After cycling, including rehydrogenation, only 14.4% $NaAlH_4$ is formed compared to the theoretical capacity of 53.9% (eq 4). This means that, even after correction for NaCl and Al formed during ball milling, the rehydrogenation is only 27% of the theoretical capacity of the first step for $NaAlH_4/Na_3AlH_6$ (eq 1), whereas the rehydrogenation of the second step (eq 2; Na_3AlH_6/NaH) is complete, because no NaH is observed. This interesting observation demands further investigation.

There is certainly enough Na_3AlH_6 available for reaction with Al. Generally, long diffusion paths, e.g. through a $NaAlH_4$ product layer, may reduce the effective capacity. However, a closer look at the Al reflections reveals that this is not the main

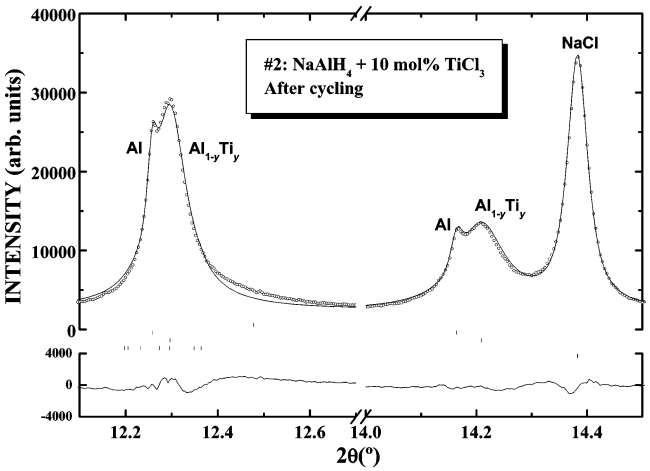

Figure 3. Observed intensities (circles) and calculated intensities from Rietveld refinements (upper line) of $NaAlH_4$ with 10 mol % $TiCl_3$ after 3 cycles, measured at 22 °C at BM1B, ESRF. Positions of Bragg reflections are shown with bars for $NaAlH_4$, Al, $Al_{1-y}Ti_y$, Na_3AlH_6, and NaCl (from top). The differences between observed and calculated intensities are shown with the bottom line.

reason in this case; cf. Figure 3. All Al reflections are split in two—a low-intensity reflection at low angles and a reflection with a significantly higher intensity at higher angles. In the earlier study with only 2 mol % $Ti(OBu)_4$, there was a shoulder at the high-angle side that was interpreted as $Al_{1-y}Ti_y$. On the basis of the unit-cell volume, y was estimated to 0.07.[11]

The low-angle reflections at 12.27 and 14.17° are in line with pure Al ($a = 4.0490$ Å). Only a small amount of pure Al is left in sample 2. If the unlikely options of amorphous or evaporated aluminum are rejected, the only reasonable possibility left is that most of the Al is chemically bonded in the phase which gives reflections at the high angle side of pure Al. Unless there is an oxygen impurity, a reaction with Ti is most likely. The extra peaks are also observed with two different additives and with increasing intensities with an increasing amount of additive.

This phase has a slightly lower unit-cell dimension than Al (4.0368 compared to 4.0490 Å) and has the same relative intensities as fcc Al. Al with small substitutions of Ti results in a smaller unit-cell dimension,[23] and the unit-cell dimensions of both the stable $D0_{22}$ and the metastable $L1_2$ modification of Al_3Ti are smaller.[18] These are indications of an Al-rich Al—Ti intermetallic phase in this case. The unit-cell volume per atom increases at the Ti-rich side of Al_3Ti to a higher value than pure Al,[18] but if the present phase had a lower Al content than Al_3Ti, then there would have been free Al both from the ball-milling reaction (eq 4) and from the fraction of Al after eq 4 which still has not reacted with Na_3AlH_6. This is not observed. Hence, the data from a sample with high additive level proves unequivocally that an $Al_{1-y}Ti_y$ phase with $y < 1/4$ is formed. If no Ti—Al phase were formed at all, an excess of Al should be present at this additive level and probably a predominant amount of Na_3AlH_6 would react.

There is no stable phase between Al and Al_3Ti according to the phase diagram,[18] and reports on fast quenching from melt results in phase separation into Al_3Ti and $Al_{0.998}Ti_{0.002}$.[23] On the other hand, there are several reports on attempts on mechanical alloying in this composition range. A continuous change in the unit-cell dimension of the more Al-rich phase with milling time from Al to approximately the unit-cell dimension of Al_3Ti has been reported.[15] Furthermore, the disappearance of Ti-reflections by PXD after ball milling has been reported.[20,21] On the basis of the quantitative phase analysis

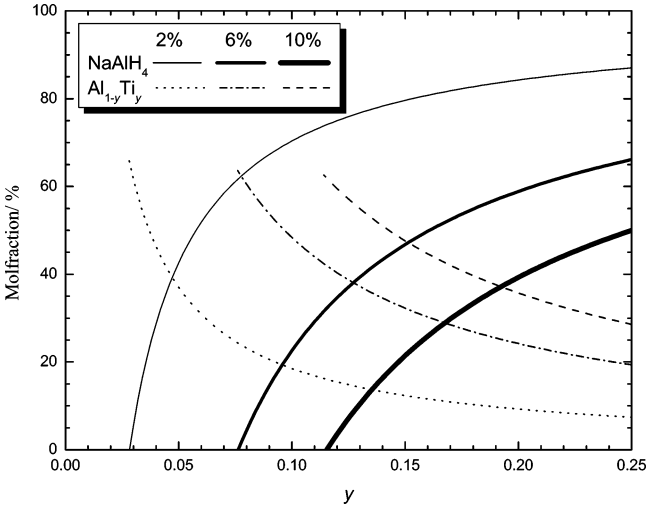

Figure 4. Mole fractions of $NaAlH_4$ and $Al_{1-y}Ti_y$ based on eq 4 for different amounts of $TiCl_3$ additive.

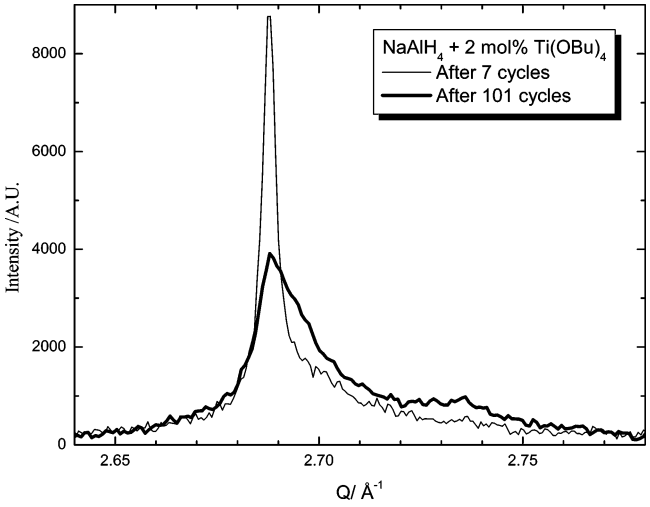

Figure 5. SR-PXD data around the strongest Al reflection for a reabsorbed sample after 7 and 101 cycles, showing that there is less free Al (left reflection) after 101 than after 7 cycles.

above, there is probably not much of the Al that reacts with Ti during ball milling even though the phases are formed in the same reaction (eq 4) and should be in close proximity in the sample. This could be due to relatively short ball-milling times used for reversible hydrogen storage in alanates compared to studies on mechanical alloying of Al−Ti intermetallics. But after a few cycles, probably because of the elevated temperature, at least a partial reaction takes place.

Apparently, the $Al_{1-y}Ti_y$ phase is so stable that Al is trapped and will not react with Na_3AlH_6. This will reduce the reversible storage capacity beyond the reduction in capacity from the dead weight from the additive and the reaction of the additive with $NaAlH_4$ during ball milling. The total reaction of the initial ball milling reaction and the formation of $Al_{1-y}Ti_y$ with $y < {}^1/_4$ during cycling could be formulated like

$$NaAlH_4 + xTiCl_3 = (1 - kx)NaAlH_4 + 3xNaCl + (x/y)Al_{1-y}Ti_y + lxNa_3AlH_6 + (2k - 3l)xH_2 \quad (6)$$

with

$$k = (3 - 6y)/2y \quad \text{and} \quad l = (1 - y)/2y - {}^3/_2$$

This equation is based on a complete consumption of all Ti in order to form a homogeneous $Al_{1-y}Ti_y$ phase. The excess Al (compared to $y = 0.25$) is taken from $NaAlH_4$, and the amount of Na_3AlH_6, with Na:Al = 3:1, is balanced to give the same amounts of Al and Ti on both sides of the equation.

A more Al-rich phase (lower y) leads to less regenerated $NaAlH_4$, as shown for 2, 6, and 10% additive level in Figure 4, and reduced capacity on the first stage of $NaAlH_4$. These curves may be used to estimate y based on the phase composition. The estimated y value is then used in the Rietveld refinements to generate new and more accurate phase compositions. By this recursive procedure a value for y is obtained. Similarly, the reduced capacities during cycling in Sieverts-type apparatus may also be used to estimate y, on the assumptions that all free Al is reacted with Na_3AlH_6 and that Na_3AlH_6 is completely dehydrided in the experimental conditions chosen for the cycling. However, reduced capacity due to reasons other than $Al_{1-y}Ti_y$ formation will lead to an underestimation of y.

The present data were used for the estimation of y. After corrections for assumed complete reaction of free Al (5.5 mol %) with Na_3AlH_6 (reversed eq 1), the remaining phase composition (to be compared to eq 6) is 22.7% $NaAlH_4$, 11.5% Na_3AlH_6, and 41.3% $Al_{1-y}Ti_y$, and the remaining is NaCl. From Figure 4, the mole fractions of $NaAlH_4$ and $Al_{1-y}Ti_y$ were used separately to estimate y values of 0.153 and 0.173. A similar curve for Na_3AlH_6 gave a y value of 0.138. The quantitative phase analysis points to the existence of $Al_{0.85}Ti_{0.15}$ in the cycled $NaAlH_4$ sample with 10% $TiCl_3$ additives. The unit-cell dimension of this Al "shoulder" is the same as that for the cycled $NaAlH_4$ sample with 2% $Ti(OBu)_4$,[11] and the composition is probably similar. The present quantitative phase analysis, based on SR-PXD, gives a more accurate composition estimate than the rough estimation from linear unit-cell volume intrapolation between Al and Al_3Ti with the $L1_2$ structure, in particular for samples with high amounts of additive. The asymmetric profile of the first $Al_{1-y}Ti_y$ reflection in Figure 3 may indicate that the composition of this phase is not completely homogeneous throughout the sample.

$NaAlH_4$ with 2 mol % $Ti(OBu)_4$ (sample 4) was in the 101th cycle re-hydrogenated at 120 °C and 86 bar pressure in a Sieverts-type apparatus with excellent temperature stability for 65 h. Of the final absorption 84 and 92% are completed during the first 12 and 20 h, respectively.

The quantitative phase analysis of this sample resulted in 71.9 mol % $NaAlH_4$, 5.9 mol % Na_3AlH_6, and 19.8 mol % Al (15.1 mol % present as $Al_{1-y}Ti_y$). In addition the sample included 2 mol % NaCl impurity. By assuming that the additive destroys 8 mol % $NaAlH_4$ and forms crystalline Al and amorphous phases such as NaOBu and Ti, the phase fractions can from eq 1 be estimated to 74.3, 5.9, and 19.8 mol %, respectively. This corresponds to 81% complete re-hydrogenation in step 1 of $NaAlH_4$.

Compared to the SR-PXD data after 7 cycles for the same sample,[11] the peak widths of $NaAlH_4$ and Na_3AlH_6 for the sample after 101 cycles are similar. However, the Al peaks differ. In Figure 5, SR-PXD data around the strongest Al peak of the 7 and 101 cycle samples are compared after background subtraction and normalizing to the strongest peak from $NaAlH_4$. Because of the slightly different wavelengths of the experiments, the data are presented on the Q-scale ($2\pi/d$). After 101 cycles the content of free Al is clearly less than after 7 cycles, probably because of the extended re-hydrogenation time. This brings about better opportunities to examine the shoulder. There appear to be two shoulders: at $a = 4.038$ Å ($Q = 2.695$ Å^{-1}) and at $a = 4.018$ Å ($Q = 2.709$ Å^{-1}). Similar double shoulders are

also observed at the high-angle side of the second strongest Al reflection. Both shoulders were included in the refinements for estimation of the fraction of $Al/Al_{1-y}Ti_y$. A possibility is that, by extended cycling, aluminum and titanium may continue the reaction and several types of Al-rich intermetallics are formed.

In the dehydrided sample after 100 cycles, the mole fractions were estimated to be 54.6, 8.7, and 35.3% Al, Na_3AlH_6, and NaH, respectively.[11] This corresponds to a 59% complete desorption of Na_3AlH_6. Since the mol fractions after the next absorption corresponds to 81%, the capacity could, as a first approximation, be estimated from the capacities of the two reaction steps to be 3.8 wt %. Corrected for the prolonged absorption in the last reabsorption, the estimation from quantitative phase analysis is close to the observed values for the last cycles, which is approximately 3.4 wt %.

4. Discussion

Three different X-ray absorption studies near the Ti edge indicate reduction of Ti^{III} to Ti^0 after the ball-milling reaction, but the interpretation of the extended X-ray absorption fine structures deviate considerably.[8−10] A general drawback of this technique is that because the Ti^0 edge is at lower energy than the edge for higher Ti valences, a smaller amount of Ti in higher valences would be masked by the Ti^0 contribution. Nevertheless, it is clear that most of the titanium precursor is reduced to the metallic state by the ball milling with the reducing agent $NaAlH_4$.

Similar results were recently shown by pressure measurements during ball milling.[24] This study showed a pressure increase in accordance with complete reduction of $TiCl_x$ to Ti. But without PXD characterization of the product, it is still a possibility for partial thermal decomposition to Na_3AlH_6 during the prolonged milling. This would eventually affect the calculated number of hydrogens released per Ti considerably.

EPR experiments, which are sensitive to Ti^{III}, show traces of Ti^{III} after ball milling with $TiCl_3$ and larger amounts of Ti^{III} after ball milling with TiF_3.[25] In both cases, Ti^{III} are replaced by signals for Ti^0 after a few cycles. This is interpreted as unreacted additive that is consumed during cycling.

The present study using quantitative phase analysis of SR-PXD data shows that ball milling of $NaAlH_4$ with $TiCl_3$ and TiF_3 leads to close to complete reaction of the Ti precursors with $NaAlH_4$, such that NaCl and Al are formed. Neither Na nor Al are found to be replaced by Ti. This implies that Ti^{III} is reduced, either partially to e.g. TiH_x or $Ti_{1-y}Al_yH_x$ or completely to Ti^0 (Ti or a Ti-rich Ti−Al alloy). Because no crystalline Ti-containing phases are found, it is not possible to conclude from SR-PXD the state of Ti directly after ball milling with $NaAlH_4$.

Recent experiments with 0.915 Ti + 0.085 Al in methanol indicate removal of pure Al within 4 h of ball milling and formation of an amorphous phase, which may contain hydrogen, after 12 h.[26] It has been reported that stable Ti−Al phases with up to 45% Al may be hydrided,[27] and metastable phases achieved by mechanical alloying up to 65% Al may be hydrided.[28] A considerable Al content would have caused a shift in the Al:NaCl ratio, which in the present work is shown to be in close agreement with eq 4 for sample 1. Similarly, a large hydrogen content in the Ti-containing phase is expected to give a shift in the near-edge X-ray absorption compared to Ti^0. These considerations indicate formation of amorphous titanium, possibly with small amounts of Al and H, after ball milling. In a recent report, a wide feature in the PXD diagram measured directly after ball milling is interpreted as an amorphous Ti−Al phase of undefined composition.[29]

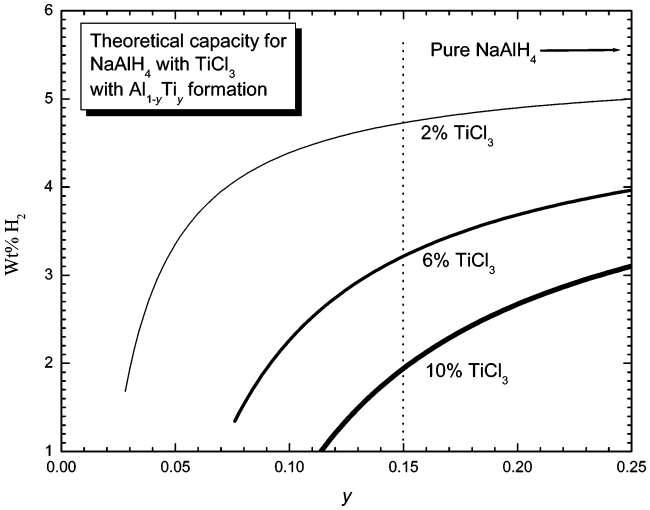

Figure 6. Theoretical hydrogen storage capacity of $NaAlH_4$ with different amounts of $TiCl_3$ additive as a function of the Ti content in $Al_{1-y}Ti_y$.

The present results show that, after cycling a metastable phase with a composition between Al_3Ti and Al is formed. This phase is formed for Ti additions as high as 10 mol %. Estimations from the quantitative phase analysis give a composition of $Al_{0.85}Ti_{0.15}$, and this phase is characterized by a unit-cell dimension of approximately 4.0365 Å, both with the $Ti(OBu)_4$ and the $TiCl_3$ additive. This phase can account for more than 80% of the Ti introduced into the sample. Furthermore, the positions of Al and Ti have been shown to be correlated in a cycled $NaAlH_4$ with TiF_3 additive from energy-dispersive X-ray analysis in a recent transmission electron microscopy study.[30]

The effect of $Al_{0.85}Ti_{0.15}$ on the kinetics of the sodium alanate system is at the moment not clear. There is always a possibility that a minor fraction of Ti is causing the improvement, whereas the major fraction is detected by PXD and other techniques. Nevertheless, after cycling Ti-enhanced $NaAlH_4$, most of the Ti is present as a solid solution in Al, and it is a reasonable possibility that Ti from this phase is of importance to the enhanced kinetics. At the moment, it is not clear whether the composition of the Al−Ti phase is constant during desorption and absorption.

When $Al_{1-y}Ti_y$ is formed during cycling, this reduces the storage capacity of the first step of $NaAlH_4$ because of insufficient Al for the reaction with Na_3AlH_6. Combined with the capacity loss from the dead weight of the additive and reaction of the additive according to eq 4, the hydrogen storage capacity of $NaAlH_4$ with $TiCl_3$ additive as a function of y in $Al_{1-y}Ti_y$ is shown in Figure 6. A decreasing y leads to a considerable loss of capacity; e.g. formation of $Al_{0.85}Ti_{0.15}$ in a sample with 2 mol % $TiCl_3$ will give a maximum storage capacity of 4.73 wt %, whereas with 10 mol % only 1.94 wt % may be maintained.

Certainly, additional decreased capacity due to long diffusion paths and resulting incomplete reaction may be important. Bogdanovic et al.[13] did observe Na_3AlH_6 after absorption, and ball milling of this sample did not remove Na_3AlH_6 completely, but excess Al added by ball milling at this stage did. This could also be interpreted on the basis of the present model, because it is reasonable to believe that ball milling does not release free Al from $Al_{1-y}Ti_y$, which probably was present in the sample

after cycling. Introduction of free Al, however, may consume the remaining Na_3AlH_6.

There are literature data available on cycling capacities for $NaAlH_4$. Bogdanovic's original data with 2 mol % $TiCl_3$ give 4.2 wt %,[1] which indicates $y = 0.10$, assuming no limitations in diffusion. Sandrock et al. studied the storage capacity as a function of additive level[2] and found a reduced capacity which corresponds to $y = 0.18$ in the framework of eq 6. These results are in the same range as the present estimation based on quantitative phase analysis.

By ball milling, it is possible to induce a variety of chemical reactions without reaching the thermodynamically most stable state; e.g. ball milling of $LiAlD_4$ and 2NaH recently has been shown to partly react to $NaAlD_4$ and LiH, which after heat treatment under pressure further reacts to $Na_2LiAlD_4H_2$.[31] Present and earlier experimental evidence indicate that mainly a redox reaction to Al^0, Ti^0, and NaCl happens during ball milling of $NaAlH_4$ and $TiCl_3$. This reaction is subsequently, during the heat treatment in the cycling, followed by another thermodynamically favorable (see e.g. ref 18) reaction: from Al and Ti to an Al-rich $Al_{1-y}Ti_y$.

Metastable Al−Ti phases are relatively stable at elevated temperature after mechanical alloying, but there is a possibility that cycling at a different temperature could give a different composition of $Al_{1-y}Ti_y$ and hence different capacity than achieved at 160 °C in the present report. The capacity of $NaAlH_4$ + 2 mol % $Ti(OBu)_4$ has, though, been shown to be quite stable at 3.5−4.0 wt % during many cycles.[3]

Acknowledgment. The skilful assistance from the project team at the Swiss−Norwegian Beam Line, ESRF, is gratefully acknowledged. S.S.S. and C.M.J. gratefully acknowledge financial support received from the Office of Hydrogen, Fuel Cells and Infrastructure Technologies of the U.S. Department of Energy.

References and Notes

(1) Bogdanovic, B.; Schwickardi, M. *J. Alloys Compd.* **1997**, *253*, 1−9.
(2) Sandrock, G.; Gross, K.; Thomas, G. *J. Alloys Compd.* **2002**, *339*, 299−308.
(3) Srinivasan, S. S.; Brinks, H. W.; Hauback, B. C.; Sun, D.; Jensen, C. M. *J. Alloys Compd.* **2004**, *377*, 283−289.
(4) Fichtner, M.; Fuhr, O.; Kircher, O.; Rothe, J. *Nanotechnology* **2003**, *14*, 778−785.
(5) Wang, P.; Jensen, C. M. *J. Phys. Chem. B* **2004**, *108*, 15827−15829.
(6) Jensen, C. M.; Zidan, R.; Mariels, N.; Hee, A.; Hagen, C. *Int. J. Hydrogen Energy* **1999**, *24*, 461−465.
(7) Bogdanovic, B.; Brand, R. A.; Marjanovic, A.; Schwickardi, M.; Tolle, J. *J. Alloys Compd.* **2000**, *302*, 36−58.
(8) Graetz, J.; Reilly, J. J.; Johnson, J.; Ignatov, A. Y.; Tyson, T. A. *Appl. Phys. Lett.* **2004**, *85*, 500−502.
(9) Léon, A.; Kircher, O.; Rothe, J.; Fichtner, M. *J. Phys. Chem. B* **2004**, *108*, 16372−16376.
(10) Felderhoff, M.; Klementiev, K.; Grunert, W.; Spliethoff, B.; Tesche, B.; von Colbe, J. M. B.; Bogdanovic, B.; Hartel, M.; Pommerin, A.; Schuth, F.; Weidenthaler, C. *Phys. Chem. Chem. Phys* **2004**, *6*, 4369−4374.
(11) Brinks, H. W.; Jensen, C. M.; Srinivasan, S. S.; Hauback, B. C.; Blanchard, D.; Murphy, K. *J. Alloys Compd.* **2004**, *376*, 215−221.
(12) Weidenthaler, C.; Pommerin, A.; Felderhoff, M.; Bogdanovic, B.; Schuth, F. *Phys. Chem. Chem. Phys* **2003**, *5*, 5149−5153.
(13) Bogdanovic, B.; Felderhoff, M.; Germann, M.; Hartel, M.; Pommerin, A.; Schuth, F.; Weidenthaler, C.; Zibrowius, B. *J. Alloys Compd.* **2003**, *350*, 246−255.
(14) Haber, J. A.; Crane, J. L.; Buhro, W. E.; Frey, C. A.; Sastry, S. M. L.; Balbach, J. J.; Conradi, M. S. *Adv. Mater.* **1996**, *8*, 163−166.
(15) Zhang, F.; Lu, L.; Lai, M. O. *J. Alloys Compd.* **2000**, *297*, 211−218.
(16) Klassen, T.; Oehring, M.; Bormann, R. *Acta Mater.* **1997**, *45*, 3935−3948.
(17) Klassen, T.; Oehring, M.; Bormann, R. *J. Mater. Res.* **1994**, *9*, 47−52.
(18) Oehring, M.; Klassen, T.; Bormann, R. *J. Mater. Res.* **1993**, *8*, 2819−2829.
(19) Oehring, M.; Yan, Z. H.; Klassen, T.; Bormann, R. *Phys. Stat. Solidi A* **1992**, *131*, 671−689.
(20) Choi, J. H.; Moon, K. I.; Kim, J. K.; Oh, Y. M.; Suh, J. H.; Kim, S. J. *J. Alloys Compd.* **2001**, *315*, 178−186.
(21) Fan, G. J.; Gao, W. N.; Quan, M. X.; Hu, Z. Q. *Mater. Lett.* **1995**, *23*, 33−37.
(22) Rodríguez-Carvajal, J. *Physica B* **1993**, *192*, 55−69.
(23) Tonejc, A.; Bonefacic, A. *Scr. Metall.* **1969**, *3*, 145−147.
(24) Bellosta von Colbe, J. M.; Bogdanovic, B.; Felderhoff, M.; Pommerin, A.; Schuth, F. *J. Alloys Compd.* **2004**, *370*, 104−109.
(25) Jensen, C. M.; Sun, D.; Srinivasan, S. S.; Wang, P.; Murphy, K.; Wang, Z.; Eberhard, M.; Naghipour, A. Unpublished results.
(26) Morales-Hernández, J.; Velázquez-Salazar, J.; García-González, L.; Espinoza-Beltrán, F. J.; Berceinas-Sánchez, J. D. O.; Munoz-Saldana, J. *J. Alloys Compd.* **2005**, *388*, 266−273.
(27) Hashi, K.; Ishikawa, K.; Aoki, K. *Met. Mater. Korea* **2001**, *7*, 175−179.
(28) Hashi, K.; Ishikawa, K.; Suzuki, K.; Aoki, K. *Mater. Trans.* **2002**, *43*, 2734−2740.
(29) Haiduc, A. G.; Stil, H. A.; Schwarz, M. A.; Paulus, P.; Geerlings, J. J. C. *J. Alloys Compd.* **2005**, *393*, 252−263.
(30) Andrei, C. M.; Walmsley, J. C.; Brinks, H. W.; Holmestad, R.; Srinivasan, S. S.; Jensen, C. M.; Hauback, B. C. *Appl. Phys. A: Mater. Sci. Process.* **2005**, *80*, 709−715.
(31) Brinks, H. W.; Hauback, B. C.; Jensen, C. M.; Zidan, R. *J. Alloys Compd.* **2005**, *392*, 27−30.